**Supporting Information**

# Optomechanical manipulation with hyperbolic metasurfaces

Aliaksandra Ivinskaya,[1,*] Natalia Kostina,[1] Alexey Proskurin,[1] Mihail I. Petrov,[1] Andrey A. Bogdanov,[1,2] Sergey Sukhov,[3,4] Alexey V. Krasavin,[5] Alina Karabchevsky,[6,7] Alexander S. Shalin,[1,8] and Pavel Ginzburg[9,10]

[1]Department of Nanophotonics and Metamaterials, ITMO University, Birzhevaja line, 14, 199034 St. Petersburg, Russia
[2]Ioffe Institute, St. Petersburg 194021, Russia
[3]CREOL, The College of Optics and Photonics, University of Central Florida, Orlando, Florida 32816, USA
[4]Kotel'nikov Institute of Radio Engineering and Electronics of Russian Academy of Sciences (Ulyanovsk branch), 48/2 Goncharov Str., 432071 Ulyanovsk, Russia
[5]Department of Physics, King's College London, Strand, London WC2R 2LS, UK
[6]Electrooptical Engineering Unit, Ben-Gurion University, Beer-Sheva, 8410501, Israel
[7]Ilse Katz Institute for Nanoscale Science & Technology, Ben-Gurion University, Beer-Sheva, 8410501, Israel
[8]Ulyanovsk State University, Lev Tolstoy Street 42, 432017 Ulyanovsk, Russia
[9]School of Electrical Engineering, Tel Aviv University, Ramat Aviv, Tel Aviv 69978, Israel
[10]Light-Matter Interaction Centre, Tel Aviv University, Tel Aviv, 69978, Israel

# Table of Content

## A. Literature review

For a particle placed over the substrate or waveguide, direction of horizontal and vertical forces might change essentially depending on the illumination scheme, particle and substrate composition as well as modes excited in the particle, bound at the interface or supported by the waveguide [1-15], see Table 1.

In the last decade a significant research effort was devoted to the studies of the optical properties of isotropic substrates. For example, Kretshmann configuration (plot (1) in Table S1), when a source is positioned below a substrate, is well studied. For dielectric substrates, for incidence angles larger than the angle of total internal reflection (TIR) the field is purely evanescent in the upper half-space. On the contrary, at smaller angles propagating harmonics are present above the dielectric substrate. In both cases for dielectric particles vertical force $F_z$ (perpendicular to the dielectric substrate) can be both repulsive or attractive [3]. For Ag particles under TIR condition repulsion or attraction to the substrate is defined by the change of the sign of particle polarizability which changes at the configuration resonance [4]. Multilayer substrates and Ag-coated dielectric beads are considered in [5]. Horizontal force (along the substrate) was shown to point in the direction of light propagation for both dielectric and Ag particles [4,5].

It was shown that a radiating dipole can be repulsed from a substrate (levitation) [6–8], plot (2) in Table S1.

In a case of a waveguide substrate (plot (3) in Table S1) [9–12], evanescent fields can cause both vertical repulsion and attraction of large particles to waveguide [9]. In horizontal direction dielectric beads can be propelled [9,10] or, vice versa, move opposite to the power flow [13] depending on the mutual orientation of phase and group velocities of a particular waveguide mode. When an illumination is incident on a substrate from the top (plot (4) in Table S1), the field is a combination of evanescent and propagating waves, and we can expect a rich variety of phenomena. Indeed, the optical force can take an arbitrary direction for large Au particles [13], while for small dielectric particles the pulling force could be achieved due to surface plasmons [14]. Enhancement of vertical forces is studied in [15]. We extend the studies of horizontal forces by exploring uniaxial anisotropic substrates (optical axis is perpendicular to interface) supporting extraordinary hyperbolic modes. Considering nanoparticles without optical resonances we can attribute optomechanical effects to the illumination scheme and modes of the substrate only.

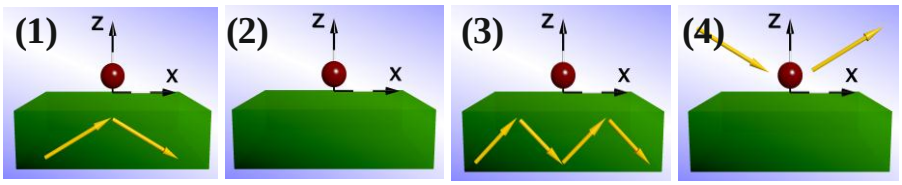


| setup | | (1) | (2) | (3) big/sm. part. | (4) |
|---|---|---|---|---|---|
| Fx | push | + | | +/+ | + |
| | pull | | | +/+ | + |
| Fz | attr. | + | + | +/+ | + |
| | rep. | + | + | +/- | + |

**Table S1.** Summary of the optical force direction for particles above the substrate. (1) Kretshmann configuration [3–5]; (2) a radiating dipole can be attracted or repulsed from the substrate even at the absence of external field [6–8]; (3) a particle above a waveguide [9–12]; (4) a particle above a substrate illuminated by a plane wave [13–15].

### B. Force calculation formalism

General expression of the force acting on a dipole particle is [16]

$$F_i = \frac{1}{2}\mathrm{Re}(\alpha \mathbf{E}^{tot} \cdot \partial_i \mathbf{E}^{tot*}), \quad \mathrm{i} = \mathrm{x}, \mathrm{y}, \mathrm{z}. \tag{S1}$$

Here we have a scalar product of the electric field vector $\mathbf{E}^{tot}$ and its derivative $\partial_i \mathbf{E}^{tot}$ along one of Cartesian coordinates, i.e. $\mathbf{E}^{tot} \cdot \partial_i \mathbf{E}^{tot} = E_x^{tot} \partial_i E_x^{tot} + E_y^{tot} \partial_i E_y^{tot} + E_z^{tot} \partial_i E_z^{tot}$. Bold capital letters stays for vector fields, capital letters with a subscript denote Cartesian components (scalar) of a vector. $\mathbf{E}^{tot}$ is the total external field at the particle location. The particle radiation self-action is included in the effective particle polarizability α obtained through the electrostatic polarizability $\alpha_{ES}$ [16]:

$$\alpha = \frac{\alpha_{ES}}{1 - i\dfrac{k_1^3}{6\pi\varepsilon_0}\alpha_{ES}}, \qquad \alpha_{ES} = 4\pi R^3 \varepsilon_0 \frac{\varepsilon - \varepsilon_1}{\varepsilon + 2\varepsilon_1}, \tag{S2}$$

where $\varepsilon_0$ and $\varepsilon_1$ are permittivities of vacuum and the upper half-space respectively, ε and R are particle permittivity and radius, $\mathbf{k}_1$ is the wave-vector in the upper half-space.

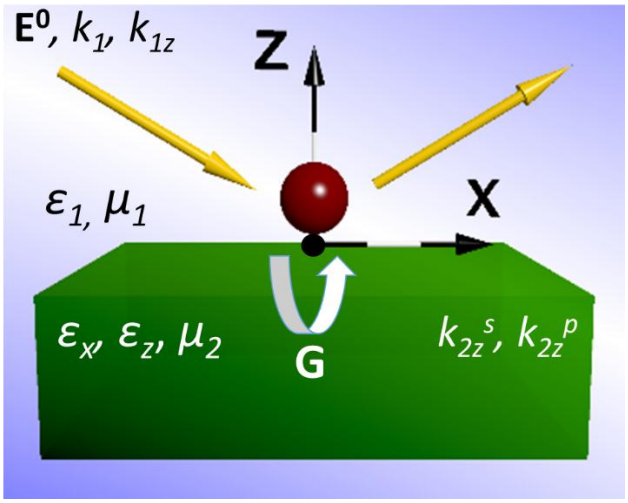


**Figure S1.** A particle of the radius R and the permittivity ε is located at the distance z above an anisotropic substrate with the permittivity components $\varepsilon_x = \varepsilon_y$, $\varepsilon_z$. The permittivity and permeability of upper half-space are $\varepsilon_1$, $\mu_1$. The origin of coordinates lies at the substrate-air interface.

If the particle is located above a substrate and illuminated by a plane wave, there are two channels constituting the field $\mathbf{E}^{tot}$ at the particle location – plane wave $\mathbf{E}^0$ (incident and reflected from the substrate) and the field scattered by the particle and reflected from substrate $\mathbf{E}^{sc,r}$. With Green's function of the reflected field:

$$\overleftrightarrow{\mathbf{G}} = \begin{bmatrix} G_{xx} & G_{xy} & G_{xz} \\ G_{yx} & G_{yy} & G_{yz} \\ G_{zx} & G_{zy} & G_{zz} \end{bmatrix}, \qquad \partial_i \overleftrightarrow{\mathbf{G}} = \begin{bmatrix} \partial_i G_{xx} & \partial_i G_{xy} & \partial_i G_{xz} \\ \partial_i G_{yx} & \partial_i G_{yy} & \partial_i G_{yz} \\ \partial_i G_{zx} & \partial_i G_{zy} & \partial_i G_{zz} \end{bmatrix}, \quad i = x, y, z, \tag{S3}$$

the field $\mathbf{E}^{sc,r}$ can be obtained as

$$\mathbf{E}^{sc,r} = \omega^2 \mu_0 \mu_1 \overleftrightarrow{\mathbf{G}} \alpha \mathbf{E}^{tot} \tag{S4}$$

where $\alpha \mathbf{E}^{tot} = \mathbf{p}$ is just an induced dipole moment of the particle. Using this expression and writing the total field $\mathbf{E}^{tot} = \mathbf{E}^0 + \mathbf{E}^{sc,r}$ at the particle location

$$\mathbf{E}^{tot} = \mathbf{E}^0 + \omega^2 \mu_0 \mu_1 \overleftrightarrow{\mathbf{G}} \alpha \mathbf{E}^{tot}, \tag{S5}$$

we can solve this equation self-consistently for the total field $\mathbf{E}^{tot}$ in the particle-substrate system taking into account multiple rescattering. With Green's function $\overleftrightarrow{\mathbf{G}}$ of the reflected field being diagonal at the dipole location, the components of the total field are given by

$$E_i^{tot} = E_i^0 (1 - \omega^2 \mu_0 \mu_1 G_{ii} \alpha)^{-1}, \quad i = x, y, z, \tag{S6}$$

where $\mu_0$ and $\mu_1$ are permeabilities of vacuum and upper half-space, $\omega$ is angular light frequency.

For evaluation of the total field $\mathbf{E}^{tot}$, Eq. S5-S6, Green's function is required. The components of $\overleftrightarrow{\mathbf{G}}$ (relevant for *p*-polarized incident wave) diagonal at the dipole location $\mathbf{r}_0$=(0,0,*z*) are [16]:

$$\begin{aligned} &G_{xx} = \frac{i}{8\pi} \int_0^\infty k_\rho \left( \frac{r_s}{k_{z_1}} - \frac{r_p k_{z_1}}{k_1^2} \right) \mathrm{e}^{-2ik_{z_1} z} \, \mathrm{d}k_\rho, \quad G_{zz} = \frac{i}{4\pi k_1^2} \int_0^\infty \frac{r_p k_\rho^3}{k_{z_1}} \mathrm{e}^{-2ik_{z_1} z} \, \mathrm{d}k_\rho, \\ &r_s = \frac{k_{1z} - k_{2z}^s}{k_{1z} + k_{2z}^s}, \quad k_{2z}^s = (\varepsilon_x k_0^2 - k_x^2)^{0.5}. \end{aligned} \tag{S7}$$

Here $r_s$ is a reflection coefficient of *s*-polarized plane wave, $k_0$ is the vacuum wavenumber, $k_{1z}$ is *z*-component of the wavevector in the upper half-space, $k_{2z}^s$ is z-component of the wavevector of *s*-polarized wave in an anisotropic substrate, $\varepsilon_x$, $\varepsilon_z$ are permittivity components of the substrate, i.e. an uniaxial crystal with the axis pointing normal to the crystal interface with air. The total field can now be found with Eqs. S6, S7 and incident field.

Finally, to obtain the final expression for the optical force, we need to differentiate Eq. S5 to find the field derivative. Field derivative relevant to $F_x$ is:

$$\partial_x \mathbf{E}^{tot} = \partial_x \mathbf{E}^0 + \omega^2 \mu_0 \mu_1 \partial_x \overleftrightarrow{\mathbf{G}} \alpha \mathbf{E}^{tot}. \tag{S8}$$

The only nonzero components of $\partial_x \overleftrightarrow{\mathbf{G}}$ are $\partial_x G_{xz} = -\partial_x G_{zx}$ which are given by Eq. 4. Then

$$\partial_x \mathbf{E}^{tot} = \begin{Bmatrix} \partial_x E_x^0 + \omega^2 \mu_0 \mu_1 \partial_x G_{xz} \alpha E_z^{tot} \\ 0 \\ \partial_x E_z^0 - \omega^2 \mu_0 \mu_1 \partial_x G_{xz} \alpha E_x^{tot} \end{Bmatrix}. \tag{S9}$$

With Eq. S9 the final expression for the optical force – Eq. 1 from the main text - is obtained.

For small distances from a substrate the imaginary part of Green's function can be approximated as

$$\mathrm{Im}\left(\partial_x G_{xz}\right)=\frac{1}{8\pi k_1^2}\mathrm{Im}\left(\int_0^\infty r_p k_\rho^3\, \mathrm{e}^{2ik_{1z}z}\,\mathrm{d}k_\rho\right)\approx\frac{1}{8\pi k_1^2}\int_0^\infty \mathrm{Im}(r_p)k_\rho^3\cos(2k_{1z}z)\,\mathrm{d}k_\rho\,. \qquad \text{(S10)}$$

### C. Green's function and excitation conditions

According to Eq. 1 a force enhancement is expected, when the term $\mathrm{Im}(\mathrm{E}_x\mathrm{E}_z^*)\,\mathrm{Im}(\partial_x G_{xz})$ is maximized. By multiplying $\mathrm{Im}(\partial_x G_{xz})$ and $\mathrm{Im}(\mathrm{E}_x\mathrm{E}_z^*)$, depicted in Fig. S1, one can see the direct correspondence to the force, which appears in Fig. 2. In line with Green's function dependence, force peak emerges only at the SPP resonance in the III quarter, while, in contrast, the negative force is achievable with a broader set of $\varepsilon_x'$, $\varepsilon_z'$ parameters in the II quadrant. In the IV quadrant, the excitation conditions give negligible $\mathrm{Im}(\mathrm{E}_x\mathrm{E}_z^*)$, prohibiting the force enhancement, despite the large values of $\mathrm{Im}(\partial_x G_{xz})$.

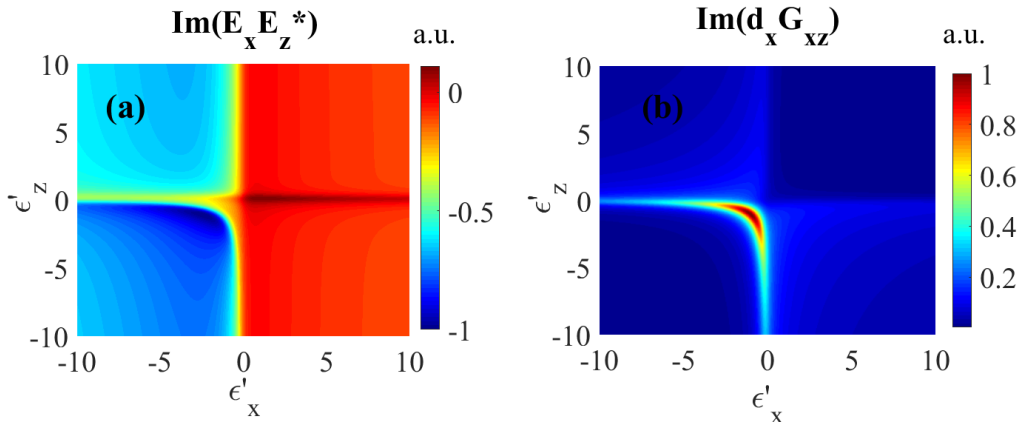


**Figure S1.** (a) The product of the field components at the particle illuminated by a plane wave, incident at 35° and (b) Green's function component $\mathrm{Im}(\partial_x G_{xz})$ for the anisotropic substrate with $\varepsilon_x'', \varepsilon_z'' = 0.3$ at coordinate $z$ = 15 nm.

In Fig. 2 (a) the highest $F_x$ is offered in the III quadrant. However, highly anisotropic metals rarely exist in nature, and such artificial materials are difficult to fabricate. As the material losses increase, anisotropic and isotropic metals in the III quadrant provide the same level of enhancement. For isotropic Ag interface ($\varepsilon'' < 0.5$), the plasmon resonance takes place at 340nm

wavelength. Metals, suitable for the operation at visible and infrared, like Au, resonate at 510 nm, and have much higher absorption. Consequently, weaker pulling forces can be achieved. Increasing the imaginary part of $\varepsilon_x''$, $\varepsilon_z''$ up to 3 and higher (the level of values, present in natural materials, e.g. Au, Cu, Al) smears out the resonance. As the result, the force enhancement, provided by surface plasmons (III quarter), become comparable with the contribution of the hyperbolic modes (II quarter).

### D. Applicability of the effective medium theory to the optical forces calculations

Straightforward investigation of the transversal force by variation of the metal fraction in the multilayer structure is shown in Fig. S2(a). The force is normalized to the intensity of an incident beam. The sharp peak around 340 nm corresponds to the surface plasmon resonance. At the visible range (relevant to experimental realizations) one can see that the multilayer substrate provides noticeable force enhancement at practically any wavelength. Figure S2(b) presents the results, obtained with the effective medium approximation.

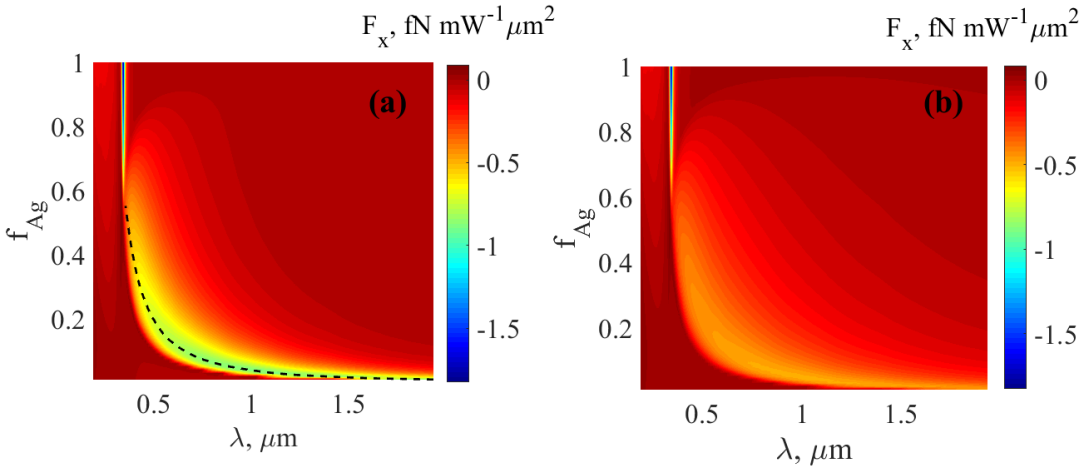


**Figure S2.** Transversal force $F_x$ acting on the particle ($R$ = 15 nm, $\varepsilon$ = 3, $z$ = 15 nm) above (a) the semi-infinite multilayer with the period $P$ = 5 nm or (b) corresponding homogenized material, as the functions of the wavelength and the metal filling factor. The multilayer is formed by Ag and a porous polymer with the top metallic layer and illuminated by a plane wave incident at 35°.

Figure S3(a) shows the peak force values (blue envelope) for multilayers with metal on the top ($P$=8 nm) along with the corresponding spectra. Figure 3S(b) compares how the same substrate

would behave if the topmost layer was dielectric (light blue line). The force drops about an order of magnitude in the case of the top dielectric layer. Metal layer thickness $d$ is plotted in the inset in Fig. S3(b) for each wavelength.

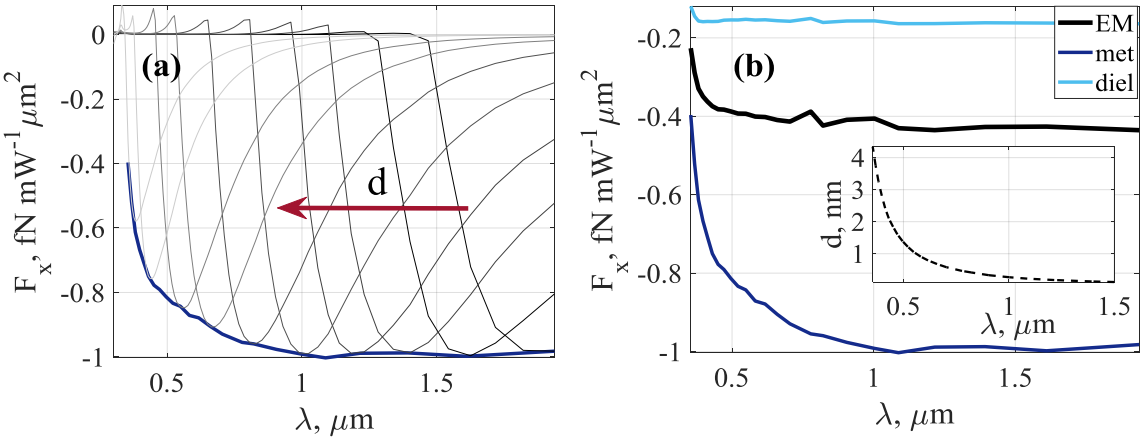


**Figure S3.** Transversal force $F_x$ acting on the particle ($R$ = 15 nm, $\varepsilon$ = 3, $z$ = 15 nm) lying on the Ag-polymer multilayer (terminating with metal) with the period $P$ = 8 nm and illuminated with a plane wave incident at 35°. (a) $F_x$ spectra for the multilayers optimized to give maximal force at each wavelength. Dark blue line (given by dashed black line in Fig. S2 (a)) is the envelope giving the peak enhancement. (b) $F_x$ envelope from (a) and analogous envelope given by the effective medium approximation (black line) and by the multilayer with the dielectric on the top (light blue line). Inset shows the metal layer thickness $d$ in the unit cell for each wavelength.

### E. Optimization of the multilayers for achieving negative optical forces

Figure S4 compares $F_x$ for different types of metal constituting multilayer, Ag, Au or Cu. For each wavelength, the multilayer is optimized to obtain the highest force values. Silver shows higher values along the spectra, especially at shorter wavelengths, where there is a drop for Au and Cu. For each wavelength the silver layer thickness $d$ giving maximal force enhancement from (a) is plotted in Fig. S4(b). The optimal $P$ for all metals is around 8-10 nm. For the smallest period the metal layer becomes thicker, what is favourable for a fabrication, while for the largest period $P$ = 12 nm $d$ decreases. At IR the vanishing metal thickness suggests that graphene could be used instead of a metal, as it was done for the $F_z$ component in [6].

Figure S4(c,d) shows the effective dielectric permittivities $\varepsilon_x$ and $\varepsilon_z$. The imaginary part of the effective permittivity in multilayers is much lower than in the case of a pure metal. As it is evident, $\varepsilon_x'$ is near-zero and negative while $\varepsilon_z'$ is positive being from 1 to 2, which corresponds to II quadrant in Fig. 2.

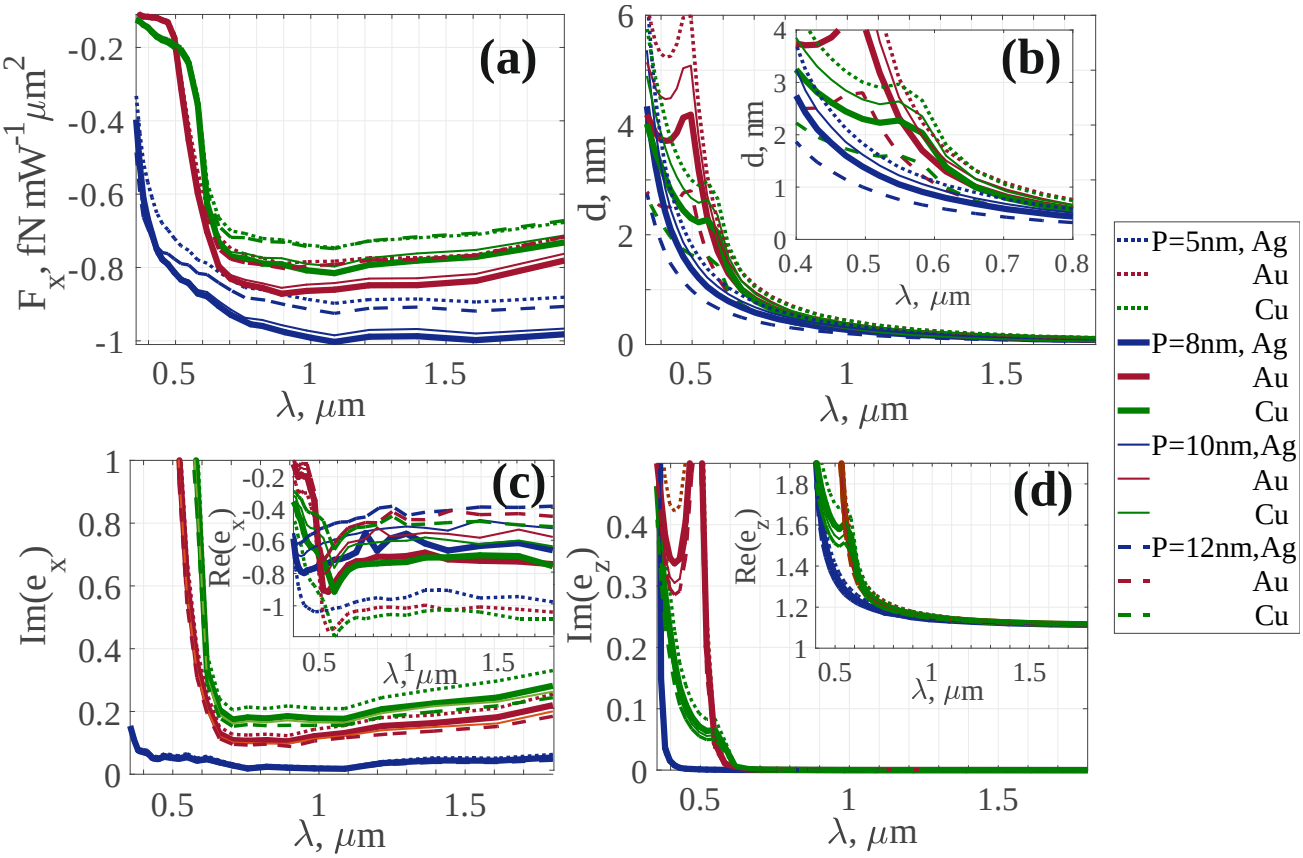


**Figure S4.** (a) Transversal force $F_x$ (optimized for each wavelength) for the particle ($R$ = 15 nm, $\varepsilon$ = 3, $z$ = 15 nm) touching multilayer with the unit cell comprising porous polymer and metal: Ag (blue color), Au (red color) or Cu (green color) with different periods (see the legend). The outer material is the metal; a plane wave is incident at 35°. The thickness of the metal layer (b) and the effective dielectric permittivities $\varepsilon_x$ (c) and $\varepsilon_z$ (d) corresponding to the optimized force values from (a).

### F. Particles suspended in water

In experimental realizations water environment is widely employed. If the upper half-space is filled with water instead of air, the effective particle polarizability given by Eq. S2 becomes smaller, and the optical force decreases. Additionally, the hyperbolic modes affect the optical force

less according to the decrease of the imaginary part of $r_p^{\infty} = (\sqrt{\varepsilon_x \varepsilon_z} - \varepsilon_1)/(\sqrt{\varepsilon_x \varepsilon_z} + \varepsilon_1)$. Figure S5 shows that in water environment optically denser particles can be used to achieve sufficient force magnitudes.

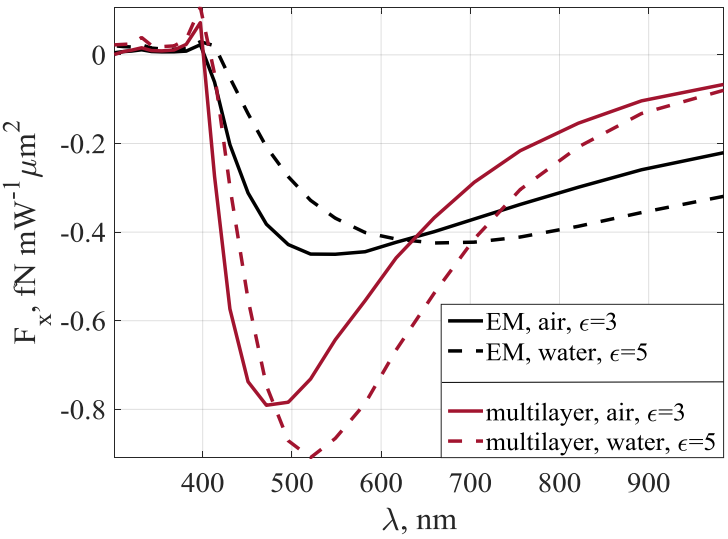


**Figure S5.** Transversal force $F_x$ acting on the particles of different permittivities, $\varepsilon = 3$ or $\varepsilon = 5$, suspended in air or water. Red lines correspond to the semi-infinite Ag-polymer multilayer ($f_1 = 0.2$) substrate with a metal layer on top and the period $P = 8$ nm. Black lines are obtained within the effective medium approach. Other parameters are: $R = 15$ nm, $z = 15$ nm, the structure is illuminated by a plane wave incident at 35°.

**References:**


[1] S. Sukhov, A. Shalin, D. Haefner, and A. Dogariu, "Actio et reactio in optical binding," *Opt. Express*, vol. 23, pp. 247–252, 2015.

[2] A. Ivinskaya, M. I. Petrov, A. A. Bogdanov, I. Shishkin, P. Ginzburg, and A. S. Shalin, "Plasmon-assisted optical trapping and anti-trapping," *Light Sci. Appl.*, vol. 6, p. e16258, 2017.

[3] P. C. Chaumet and M. Nieto-Vesperinas, "Coupled Dipole Method Determination of the Electromagnetic Force on a Particle over a Flat Dielectric Substrate," *Phys. Rev. B*, vol. 61, pp. 14119–14127, 2000.

[4] J. R. Arias-Gonzalez and M. Nieto-Vesperinas, "Optical forces on small particles: attractive

and repulsive nature and plasmon-resonance conditions," *J. Opt. Soc. Am. A*, vol. 20, pp. 1201–1209, 2003.

[5] Y. G. Song, B. M. Han, and S. Chang, "Force of surface plasmon-coupled evanescent fields on Mie particles," *Opt. Commun.*, vol. 198, pp. 7–19, 2001.

[6] F. J. Rodríguez-Fortuño and A. V. Zayats, "Repulsion of polarised particles from anisotropic materials with a near-zero permittivity component," *Light Sci. Appl.*, vol. 5, p. e16022, 2015.

[7] F. J. Rodriguez-Fortuno, A. Vakil, and N. Engheta, "Electric levitation using eps-near-zero metamaterials," *Phys. Rev. Lett.*, vol. 112, p. 33902, 2014.

[8] S. Krasikov, I. V. Iorsh, A. Shalin, and P. A. Belov, "Levitation of finite-size electric dipole over epsilon-near-zero metamaterial," *Phys. Status Solidi - Rapid Res. Lett. - Rapid Res. Lett.*, vol. 8, pp. 1015–1018, 2014.

[9] H. Y. Jaising and O. G. Hellesø, "Radiation forces on a Mie particle in the evanescent field of an optical waveguide," *Opt. Commun.*, vol. 246, pp. 373–383, 2005.

[10] L. N. Ng, B. J. Luff, M. N. Zervas, and J. S. Wilkinson, "Propulsion of gold nanoparticles on optical waveguides," *Opt. Commun.*, vol. 208, pp. 117–124, 2002.

[11] V. Intaraprasonk and S. Fan, "Optical pulling force and conveyor belt effect in resonator-waveguide system.," *Opt. Lett.*, vol. 38, pp. 3264–3267, 2013.

[12] A. V. Maslov, "Resonant pulling of a microparticle using a backward surface wave," *Phys. Rev. Lett.*, vol. 112, pp. 113903-1–5, 2014.

[13] M. M. Salary and H. Mosallaei, "Tailoring optical forces for nanoparticle manipulation on layered substrates," *Phys. Rev. B*, vol. 35410, pp. 35410–16, 2016.

[14] M. I. Petrov, S. V Sukhov, A. A. Bogdanov, A. S. Shalin, and A. Dogariu, "Surface plasmon polariton assisted optical pulling force," *Laser Photon. Rev.*, vol. 10, pp. 116–122, 2016.

[15] S. Wang and C. T. Chan, "Strong optical force acting on a dipolar particle over a multilayer substrate," *Opt. Express*, vol. 24, pp. 2235–2241, 2016.

[16] L. Novotny and B. Hecht, *Principles of Nano-Optics*, 2nd ed. Cambridge University Press, 2012.